Development of a Miniature High Frequency Ventilator for Genetically Engineered Newborn Mice

by

Kumaran Kolandaivelu

Submitted to the Department of Mechanical Engineering
in Partial Fulfillment of the Requirements for the Degree of

Bachelor of Science in Mechanical Engineering

MASSACHUSETTS INSTITUTE OF TECHNOLOGY

August 1995

Author .....
Department of Mechanical Engineering
August 1995

Certified by .....
Dr. Chi-Sang Poon
Harvard-MIT division of Health, Science and Technology
Thesis Supervisor

Accepted by .....
Prof. Peter Griffith
Senior Registration Officer

Development of a Miniature High Frequency Ventilator for Genetically Engineered Newborn Mice

by

Kumaran Kolandaivelu

Dr.Chi-Sang Poon, Thesis Supervisor

Abstract

The need for a mechanical device to assist in newborn mouse respiration has arisen from recent studies on NMDA deficient mutants. These animals die within 10-20 hours after birth, making further studies into the role of the NMDA receptors in neural plasticity and development impossible. Experimental investigations have revealed a probable cause of death to be respiratory failure.

As a first step toward prolonging the lives of the mutants, a miniature high frequency ventilator was developed to aid respiration. Since such ventilatory attempts have never been made, the device was allowed a large specification range (pressure from 0 to 25 cm H20/ frequency from 0 to 50 Hz) which would allow for both normal (low frequency, high pressure) and high frequency (high frequency, low pressure) operations. A performance study revealed that the ventilator operates well over the desired pressure range for frequencies up to 50 Hz.

Initial in-vivo studies on the mutants have revealed that the life span can be increased with respiratory assistance by at least 10 hours. In conjunction with drug therapy and maintenance efforts (feeding and thermoregulation), the life expectancy of the mutants is likely to further increase. Additional studies are currently being performed to further understand the techniques and role of newborn mouse ventilation.

Table of Contents

Chapter 1

Introduction

1.1 Need for Newborn Mouse Ventilation

Genetically engineered mice, made possible by techniques of molecular biology, are a valuable resource in furthering both the medical and biological sciences. By changing the chromosomal content in specific ways, various proteins can be knocked out or altered, whose expression or lack thereof can be investigated. The mice are a choice animal for such studies. Presently, much of their genome has been mapped. Additionally, like humans, they are mammals and therefore share many homologous chromosomes. By studying mice, further insight into human function can be gained. Furthermore, the mice can be bred with regularity and ease.

Unfortunately, the phenotypical expression of mutations can sometimes be detrimental to the well-being of the mice. Various problems such as cardiac or respiratory failure can occur, causing premature death. Presently, there is no equipment designed to sustain newborn animals of this size, and such problems go unsolved in many laboratories.

The need for a miniature mechanical ventilator for newborn mice has arisen from recent studies on NMDA-R1 genetically engineered mice. The NMDA-R1 subunit is a key component of NMDA receptors. These receptors are believed to play a critical role in the plasticity of the nervous system. Unfortunately, the mice die within the first 10 to 20 hours after birth -- prior to most major neurological developments -- precluding further studies into the role of NMDA receptors in learning and memory [1,2].

The recessive mutation has various side effects. Some studied abnormalities include loss of hind leg motor control and balance, improper mastication (leading to an inability to suckle milk), and a degradation of the respiratory system. Observation of these symptoms has proven to be an effective determinant of the genetic makeup (either homozygous recessive, or homozygous/heterozygous dominant) when compared to genetic prototyping data.

Previous studies have shown that the respiratory failure is in the NMDA-R1 knockout mice preceded by periods of apnea and respiratory instability (see figure 1). One hypothesis that has been raised is that the early deaths of the newborn mutants are caused by such respiratory failure.

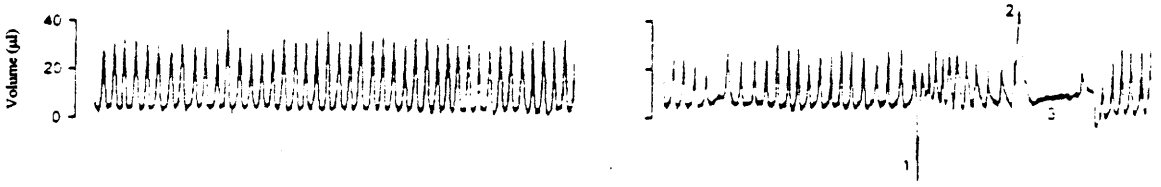

Figure 1: Breathing samples for newborn mice. a. Normal b. Control

By artificially ventilating the knockout mice, the respiratory system may be preserved. This may prolong the lives of the mice for a more thorough study into the roles of the NMDA receptors in neuroplasticity and neural development.

1.2 Current Ventilator Methods

Current animal ventilators are not suitable to ventilate neonatal mice. They are designed to deliver positive pressure at the airways via pistons, diaphragms, or pressure

sources. Being designed for larger animals, the devices generally deliver volumes of at least a few milliliters. Previous studies have shown that the newborn mice have tidal volumes ranging from .015 to .045 ml. Existing devices would therefore be imprecise over the required range. Such unreliability could result in uncontrolled volume generation and barotrauma for the fragile newborns.

A further problem with the current ventilators is that creating a positive pressure at the airway generally requires an intratracheal connection. Though this surgical procedure can be performed with some confidence in larger animals, a tracheotomy is too difficult to perform on newborn mice. Generally, this technique requires opening the throat and inserting a tube into the thrachea-- an extremely invasive operation considering the size and fragility of the neonates. Such trauma makes the use of this ventilatory style an impossibility in the mutant mice.

A final concern with current methods of animal mechanical respiration is that the ventilators deliver automatic breaths at regular intervals. Such mechanically controlled breathing creates a problem, especially since the knockout mice breathe over a wide range of frequencies. The normal frequency is about 120 breaths per minute (bpm). However, depending on the stage of respiratory distress, much lower frequencies (60 bpm) have been observed [3]. Delivering automatic breaths at a significantly different frequency than the spontaneous rate can be uncomfortable, and moreover, may provoke ventilator fighting by the animals. This condition arises when some of the animal breaths are out of phase with the mechanical breaths (i.e. the animal expires while the ventilator gives a positive inspiratory pressure).

The competing efforts result in a decrease in the ventilatory efficiency and can cause further respiratory trauma to the already sick animal.

1.3 Strategies for Improvement

To minimize the invasiveness of the subject/ventilator connection and reduce the risk of barotrauma, a negative pressure strategy can be employed. Instead of creating positive airway pressure, a negative pressure is generated around the body surface (see figure 2).

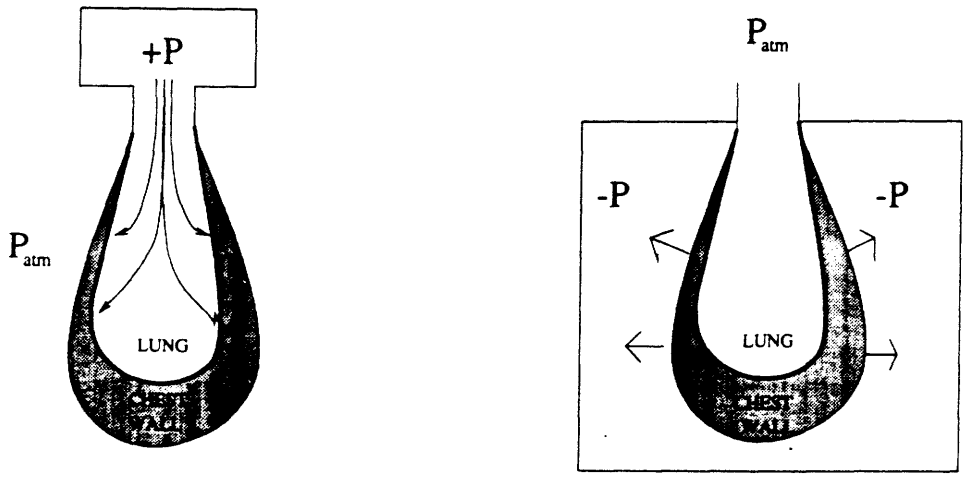

Figure 2: Methods of ventilation. a. Positive pressure b. Negative pressure

Such techniques were used on humans in the 1950s and 60's with devices aptly named 'iron-lungs.' These machines were bulky and inefficient, and therefore were quickly outmoded with the advent of positive pressure respirators. However, studies have shown

thoracic oscillations to be as effective as tracheal methods in allowing blood gas exchange [4]. An advantage of the negative pressure technique for newborn mouse ventilation is that the only physical connection to the subject is an external cuff around the neck to isolate the body from atmospheric pressure.

Two methods to overcome the problem of ventilator fighting are through patient triggered systems, such as pressure support and negative impedance ventilation [5,6], or through high frequency ventilation (HFV).

For human ventilation, patient triggering systems have been developed, where the breathing effort of a patient can be sensed via pressure or flow fluctuations. The effort is then assisted with an inspirtory pressure. Unfortunately, the pressures and flows generated by a newborn mouse are too minute to be sensed reliably. A high threshold would mean a significant time delay in respiratory assistance, while a low threshold would result in excess breathing due to noise.

High frequency ventilation considers an alternate method of breathing by fluctuating respiratory pressures at several times the normal frequency in the range of 10 to 30 Hz. To prevent over-ventilation and hypocapnia, the tidal volume is accordingly reduced by an order of magnitude. This process results in simply oscillating the air within the lungs. Previous studies performed on larger animals have revealed that HFV provides adequate gas exchange in the alveoli, and is therefore an effective method of ventilation [7].

With these considerations, a miniature HF negative pressure ventilator was developed. HF oscillators used on rats have proven to be an effective means of

ventilation. However, the small size and frahility of the newborn mice creates a more complex problem. Since such minute volumes are generated, the leakage in the system must be minimized in a non-invasive manner. Also, the previous system applied both a positive and negative pressure to the body surface,. with a mean pressure equal to atmospheric [4]. Although such pressure fluctuations are acceptable in small volume generation (in comparison with the tidal volume), if larger volumes are needed, the positive surface pressure could pose a serious threat to the subject by constricting airways.

Since mechanical respiratory attempts have never been made on newborn mice, a large specification range was needed. The ventilator was designed to deliver volumes from 0.00 ml to 0.04 ml over a frequency band of 1 Hz (in the normal range) to 100 Hz (higher than the present limits of HFV).

1.4 Organization of Thesis

This paper is divided into four major sections. Chapter 2 deals with the ventilator design. First, an over all illustration is given and divided into the major subassemblies. Each assembly is described both physically and theoretically. The performance of the developed prototype is then discussed in chapter 3. The evaluation is split into strict mechanical operation, and in-vivo studies performed on actual mutants. Chapter 4 summarizes the design and performance, and gives insight into future modifications. Finally, the theoretical model simulations are included in the Appendices, along with extra data on the actuator system.

Chapter 2

Design

2.1 Overview

Figure 3 shows a full schematic of the mechanical ventilator design. The device has four major subsections: the pressure generating piston assembly, the pressure normalizing valve assembly, the motor and controller, and the mouse chamber. Each assembly is discussed in detail in the following sections.

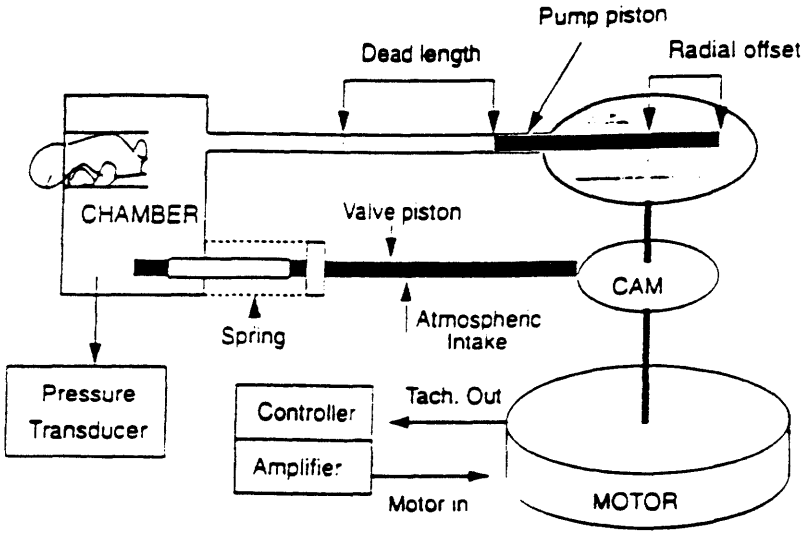

Figure 3: Schematic diagram of ventilator design

2.2 Pressure generating piston assembly

2.2.1 Description

Figure 4 shows a schematic of the pressure generating assembly. It consists of a piston hinged at one end via flexible tubing, and to a radially adjustable pin mounted on a

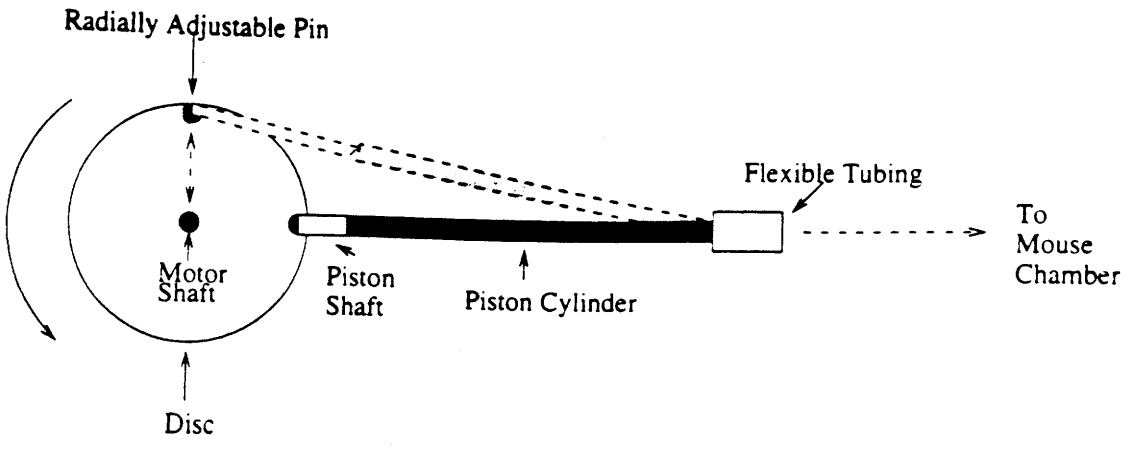

Figure 4: Schematic of pressure generating piston assembly

6 cm diameter aluminum disc at the other. The piston comprises a 10 cm long brass shaft with an outer diameter of .49 cm sliding in a 9 cm long brass cylinder with an inner diameter of .51 cm. The piston head is attached to the adjustable pin which can move radially on a screw track. Since the other end of the piston is fixed translationally by the flexible tubing, the radial adjustment allows the stroke length of the piston to be varied by the simple relation:

$$\text{Stroke} = 2 * \text{Radial location} \qquad (1)$$

The aluminum disk is press fit to a 3 mm axle. By rotating the disk at a constant velocity, the piston cycles in a sinusoidal motion given by :

$$x = x_0 \sin(wt) \qquad (2)$$

where x is the piston position, xo is the radial offset, w is the disk angular frequency, and t is time.

2.2.2 Methodology

In order to find the dimensions of the piston assembly, the required pressure swing that needed to be generated in order to create tidal volumes from 0.00 ml to 0.04 ml were found. Obviously, a 0 ml volume translates to a 0 cm H20 pressure variation. To find the upper pressure limit, the mechanical nature of the newborn mouse respiratory system was considered.

The system can be modeled by the following electrical circuit:

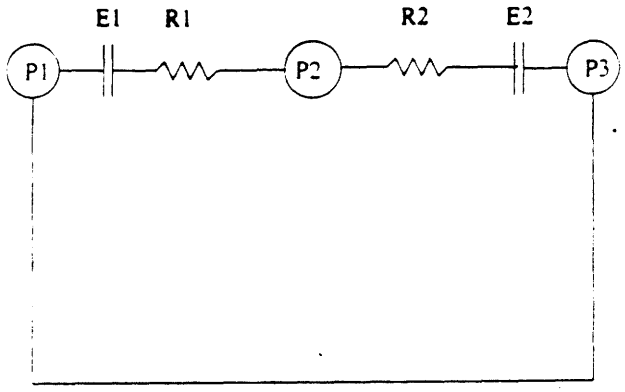

Figure 5: Electrical model of respiratory system

where P1 represents the external pressure and chest wall effort (assumed to be zero if the animal is not breathing), P2 is the pleural pressure, and P3 is the airway pressure. R1 and E1 are the resistive and elastic parameters of the chest wall respectively, and R2 and E2 are the similar parameters for the lung and airways. Since the goal of negative pressure ventilation is to vary P1 in order to generate a volume, P2 is of no consequence. This allows R1 and R2 to be lumped into a total respiratory resistance, Rt, and E1 and E2 into a total elastance, Et.

The governing differential equation for this simplified system is:

$$R_t q + E_t \int_{t1}^{t2} q = P1 + P3 \qquad (3)$$

where q is the flow through the system, t1 is the time at the start of inspiration, and t2 is the end inspiratory time. The integrated flow term over an inspirtory cycle represents the tidal volume. For negative pressure ventilation, P3 remains constant at atmospheric pressure.

The parameters Rt and Et were estimated using general scaleable equations for mammals:

$$R_t = 24.4m^{-.70} \qquad (4a)$$

$$E_t = \frac{1}{1.56m^{1.04}} \qquad (4b)$$

where m is the mass of the mammal in kg [8]. Using an average newborn mass of .0015 kg from previous studies, Rt and Et were determined to be 2.31 cm H20/(l/sec) and 554 ml/cm H20 respectively.

The desired tidal volume is given to be 0.04 ml in equation 3. Therefore, assuming P1 to be a sinusoidal negative gauge pressure (as would be generated by a piston motion described in equation 2), a simple program was written to numerically solve equation 3 using Euler's method (see Appendix A). By giving the amplitude of the pressure swing, the flow and tidal volume were found for a single inspiratory cycle. The process was iterated using different pressure amplitudes until the desired tidal volume was attained. The pressure range for the pressure generating piston was determined to be from 0 to 25 cm H20 (though a pressure of 22.8 cm H20 was sufficient to generate to .04 ml tidal volume).

The assembly dimensions were found by constructing a mathematical model of the piston system. The model assumed that the air behaved as an isothermal ideal gas governed by the ideal gas law:

$$PV = mRT \tag{5}$$

where V is the volume of the body cavity isolation chamber, P is the absolute pressure in the chamber, R is the gas constant (287 J/kgK for air), m is the mass of air in the chamber, and T is the air temperature. As the piston oscillates, the pressure, volume and mass can vary, though the temperature is constant, due to the isothermal assumption. Therefore, equation 5 can be expressed in a more useful differential form:

$$dP = \frac{dmRT - PdV}{V} \tag{6}$$

The volume change, dV, is described by the equation:

$$dV = \dot{x}\pi r^2 \tag{7}$$

where $\dot{x}$ is the time derivative of the piston position, x, or velocity, and r is the radius of the piston. As seen in equation 2, the general piston motion is sinusoidal. However, to describe the actual motion, the phase and equilibrium position must be determined from the initial conditions. The piston starts in a compressed state, and rotates, generating a negative pressure until fully extended (the stroke length). Considering these conditions, the piston motion is:

$$x = x_0 - x_0 \cos(wt) \tag{8a}$$

$$\dot{x} = dx \tag{8b}$$

$$= wx_o \sin(wt) \tag{8c}$$

The change in mass, dm, in equation 6, can be determined from fluid flow considerations. Combining the Cuvette and Pousille flow equations [9], the relation:

$$dm = 2\rho\pi r\left[\frac{dxh}{2} - \frac{h^3(P_{gauge})}{12\mu a}\right] \tag{9}$$

is found, where ρ is the density of air (1.204 kg/m^3), μ is the viscosity of air (1.82e-5 Pas), Pgauge is the gauge chamber pressure, r is the average piston radius (shaft and cylinder), h is the gap size between the piston shaft and cylinder, and l is the length of the gap, geometrically related to the piston motion by:

$$a = 2x_0 + a_0 - x \tag{10}$$

where ao is the nominal length of the piston shaft in the cylinder at all times during maximal stroke. The first bracketed term in equation 9 is a result of mass transfer due to the generated pressure gradient across the gap while the second term is the leakage caused by the relative motion between the piston shaft and cylinder wall. The first term dominates equation 9 due to air's low viscosity.

The theoretical model described by equations 6, 7, 8b, c, and 9 was then numerically solved using a pre-defined 3rd order Runga Kutta function (ODE23) available in MATLAB (the program listing is given in Appendix B). The variables that could be adjusted were the stroke length, the shaft radius and length, the cylinder radius and length, and the volume of the mouse chamber. Each parameter needed to be considered in order to determine suitable dimensions.

The shaft/cylinder gap size (ideally 0 for no leakage), was limited by achievable tolerances and cost considerations. Another concern was that the stroke length needed to

be small (due to size concerns and jamming problems dependent on the piston length), yet large enough for discernible radial piston positions to allow the pressure to be varied accurately between the 0 to 25 cm H20 range. Finally, by making the shaft and cylinder longer than the stroke length (thereby lengthening the gap), the leakage could be reduced by increasing resistance to Pousille flow. Again, the lengths could not be too long, for practical considerations.

With these limitations, the piston radius and chamber volume were adjusted to ensure the maximum pressure of 25 cm H20 could be achieved. After several runs, suitable parameters were obtained (piston shaft radius=.00245m/ piston cylinder radius=.00255m/ stroke length=3cm/ nominal gap length=5cm/ chamber volume=15 ml). Some example runs are shown in figures 6, 7 and 8.

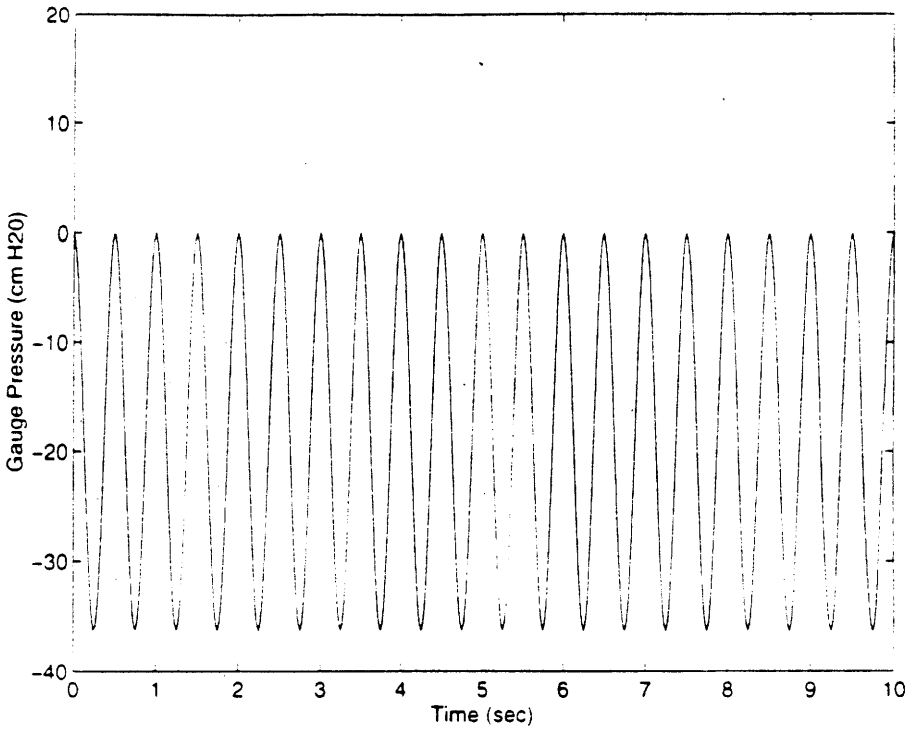

Figure 6: Theoretical pressure profile for 0.0 cm gap (no leakage)

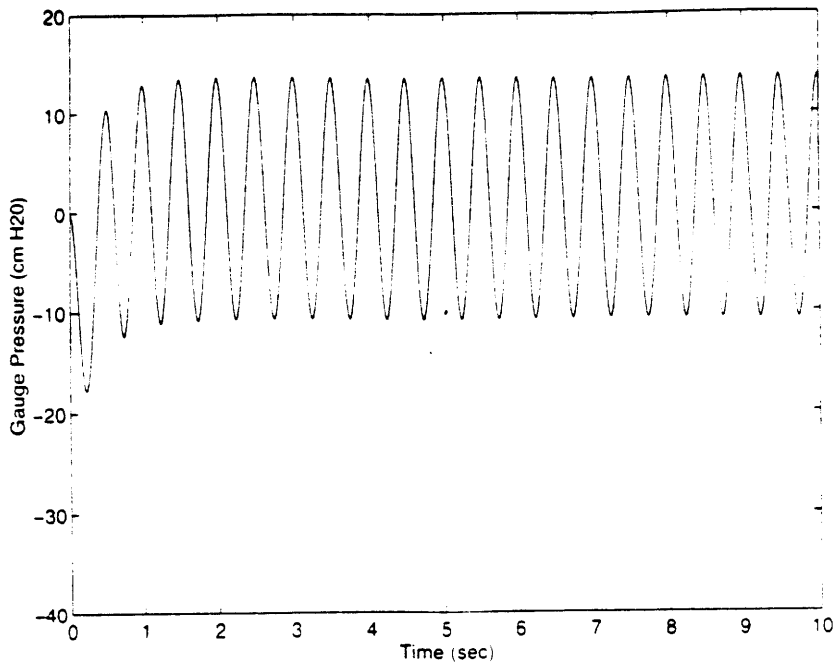

Figure 7: Theoretical pressure profile with 0.08cm gap (high leakage)

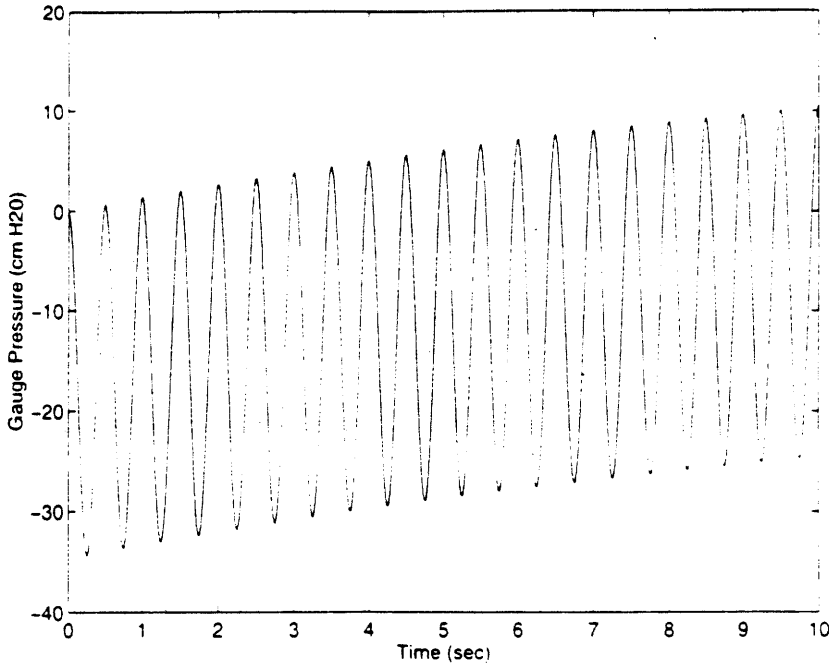

Figure 8: Theoretical pressure profile for 0.03 cm gap (low leakage)

Figure 6 depicts an unrealistic simulation with no gap, and therefore, no leakage. The pressure starts at 0 cm H20 gauge pressure (one atmosphere) and drops to 37 cm H20, before rebounding back to the base-line. Figure 7, on the other hand, has a large gap, of .08 cm. As the negative pressure is generated, leakage causes mass to be transferred into the chamber. Therefore, when the piston rebounds, a positive pressure is generated, causing the subsequent swing to start from an elevated level. With a large gap, this base-line shift settles quickly as the gauge pressure osciliates about 0 cm H20. The maximum pressure swing achieved is 18 cm H20, over half that of the no gap case. Since all systemic leakage was not modeled, it is clear that the piston must be over-designed to ensure the full 25 cm H20 specification can be met. Finally, figure 8 shows a realistic simulation, with a .02 cm gap. The pressure in the first few oscillations closely resembles the no gap case. Unavoidable, there is still a pressure drift, though it has a much longer time constant than the large gap scenario. The base-line shift lead to the development of a pressure normalizing valve, as described in the following section.

2.3 Pressure normalizing valve assembly

2.3.1 Description

A schematic of the normalizing valve can be seen in figure 9. The components include a cam and a .49 cm outer diameter hollow shaft closed at both ends. The shaft is concentric with a .51 cm cylindrical port extending .7 cm into the mouse chamber. The camshaft has an inlet slit .7 cm from the end proximal to the mouse chamber and another outlet on the length of shaft outside the chamber. The cam, which is coaxial to the

pressure generating piston disk, drives the shaft providing a .7 cm stroke. The cam has been designed to provide the maximal stroke through out the entire positive pressure phase of the pressure generating piston, while retracting during the negative phase. This action allows the mouse pressure to equilibrate with atmospheric pressure throughout the positive phase.

A cam follower (essentially a flat surface perpendicular to the shaft) provides the contact surface between the shaft and cam. The follower is guided by tracks to keep undesirable force components from bending the shaft. A 986 N/m spring holds the cam follower in contact with the cam perimeter.

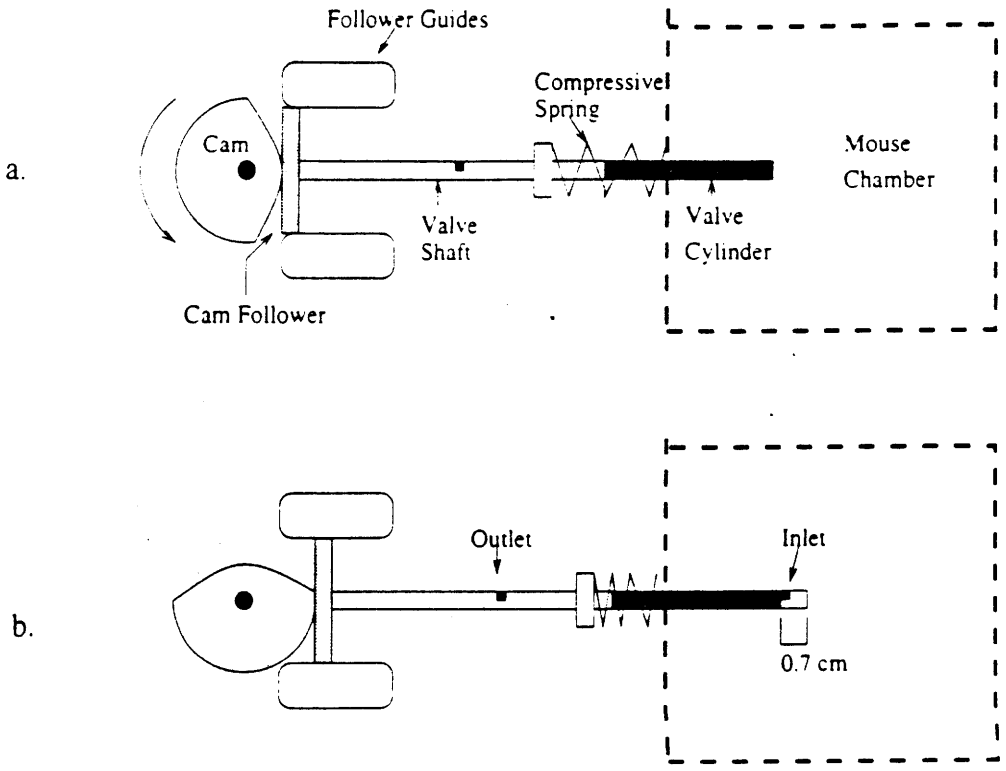

Figure 9: Schematic for normalizing valve assembly. a: Closed b: Open

2.3.2 Methodology

The need for the valve normalizing piston is evident in figures 6-8. As figure 8 indicates, even with low leakage, there is an unavoidable pressure drift due to leakage in the system. Additionally, the simulations deal with leakage through the piston gap, though there are undoubtedly other problematic areas, such as the ventilator/mouse connection

The pressure drift is detrimental in two ways. Firstly, the upward shift means the desired negative pressure cannot be reached without changing the piston parameters (seen in figure 7). More importantly, the positive pressure generated, which upon equilibration is equal in magnitude to the negative pressure, serves to compress the body cavity, thereby closing the subject's airways. Such an effect is detrimental to any ventilatory efforts.

In larger ventilators, the leakage is not a major concern since the volumes dealt with are much larger than the mass transfer due to leakage. However, the small volume needed for neonatal mouse respiration necessitates that the leakage problem be considered.

In order to eliminate the effects of mass transfer, the chamber pressure must be normalized with each cycle. Two methods considered were the cam valve design and a solenoid valve mechanism. The solenoid was rejected since it would require the use of additional actuators, increasing the system complexity. Also, such a mechanism would need a triggering cam similar to the present design. Therefore, to minimize complexity and redundancy, the cam valve method was chosen.

The cam was designed to have a maximum outer radius of 2 cm, equal to the maximum radial offset of the pressure piston (a 4 cm stroke was allowed for the prototype

design). This guaranteed size consistency regardless of later design changes. Another requirement was the cam stroke needed to be as large as possible in order to minimize leakage through the normalizing valve slit during the negative pressure swing (the larger the stroke, the further the slit could be placed from the chamber end, thereby increasing resistance to mass transfer). The limiting factor on the stroke length, other than the overall size limit of 2 cm on the cam radius, was the pressure angle. The pressure angle is defined as the angle between a line normal to the cam follower trace (essentially the cam surface) and the line drawn from the cam's center to the cam/follower contact point. A large pressure angle creates significant torque on the camshaft, resulting in inefficiency, and therefore is generally limited to under 30^{o} [10]. Two possible cam designs, one with a base circle of 1.3 cm (stroke of .7 cm) and one with a circle of 0.8 cm (stroke 1.2 cm) are shown in figures 10a and b. The pressure angle profiles for the cams were determined geometrically and are presented in figure 11. The first cam, represented by the solid line, has a maximum pressure angle of just under the 30^{o} limit (28.5^{o}) . The second cam (dashed line) has a pressure angle exceeding the given limit (45^{o}). After such considerations, the first design was selected. A displacement profile of the chosen cam is given in figure 12.

Another design consideration in the pressure normalizing valve assembly was the spring. A spring with a sufficiently large spring constant was required to ensure the cam follower would remain in contact with the cam surface. Such selection would reduce the chattering and wear of the cam assembly, and more over, keep the valve timing in synchronization with the pressure generating piston.

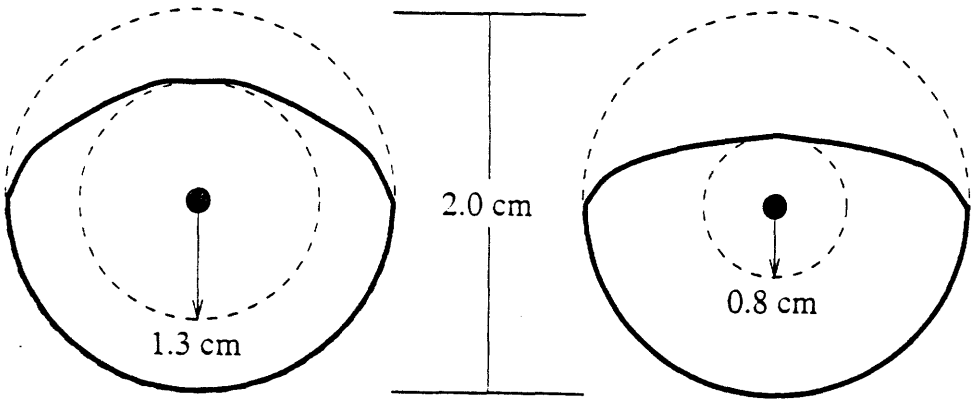

a. b.

Figure 10: Two cam designs a: 1.3 cm base circle. b: 0.8 cm base circle

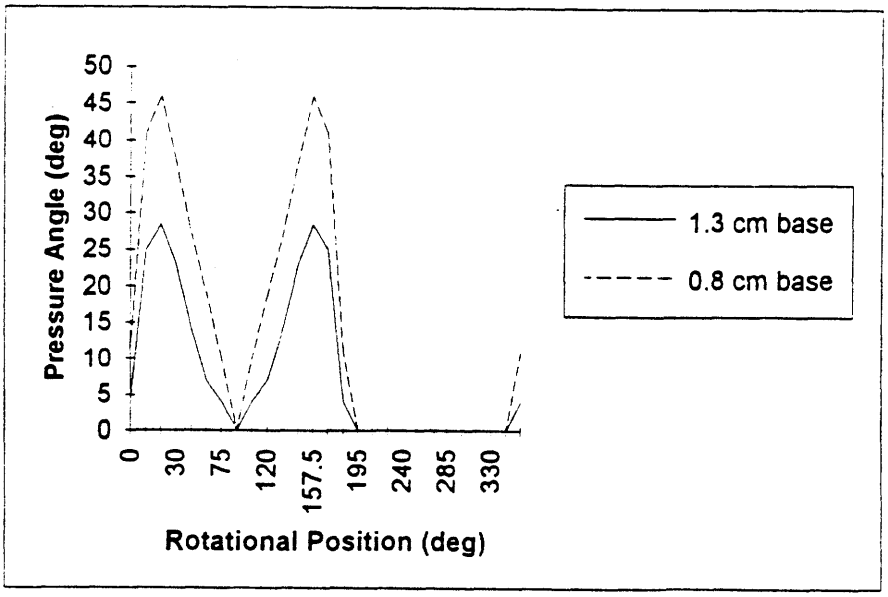

Figure 11: Pressure angle profiles for various cam designs (1.3 cm and 0.8 cm base circle)

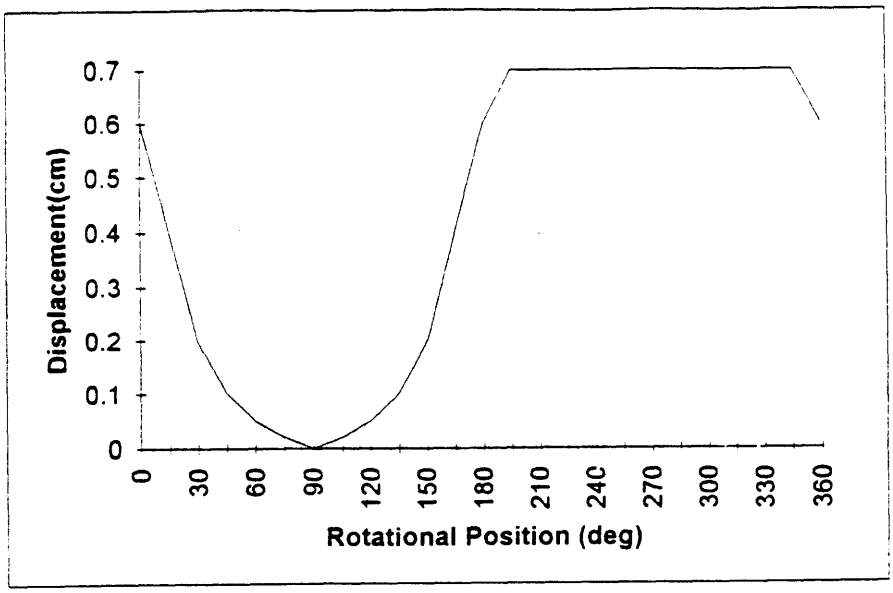

Figure 12: Displacement profile of selected .7 cm stroke cam

To find the proper spring, the natural frequency of the valve assembly was found by the relation:

$$w_n = \sqrt{\frac{k}{m}} \qquad (11)$$

where k is the spring constant and m is the mass of the moving shaft and cam foliower. The maximum frequency was known to be 628 rad/sec (100 Hz) and the mass was .01 kg, Therefore, k was 3950 N/m. Since the 100 Hz was an extreme limit, it was decided to tailor the spring for 50 Hz speed resulting in a 986 N/m spring constant. This would enable higher speeds to be achieved, though chattering would occur. However, it would also decrease the energy needed to drive to system considerably (as seen in the next section).

The next step was to determine a motor which could actuate the piston and cam assemblies.

2.4 Motor/ Controller

2.4.1 Description

A schematic of the actuator system is shown in figure 13. The actuator used to drive the ventilator is a KOLLMORGAN U9M4T servobrush motor. It is velocity controlled with tachometer feedback by a KXA-48 amplifier. The system is powered by a 48V/8 amp power transformer. The motor shaft is connected to a 3 mm steel shaft which drives the cam and pressure piston assemblies via an aluminum joiner. Both shafts are press fit in the joiner and held snugly with screws. The 3 mm shaft rotates in two greased ball bearings that are separated by 2 cm.

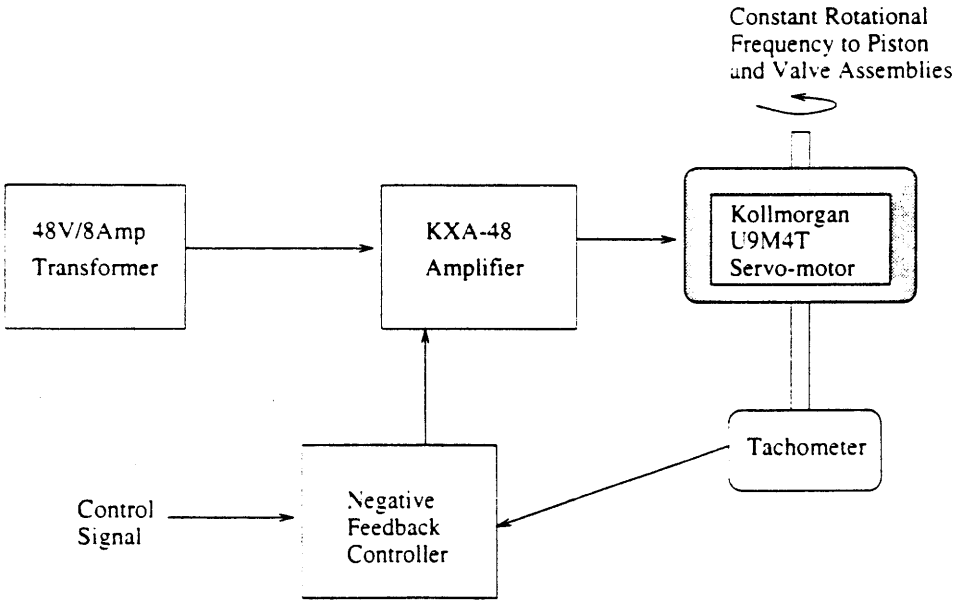

Figure 13: Schematic of motor/controller system

2.4.2 Methodology

Motor selection depended on the ability to provide adequate torque over the 0-100 Hz operating range. In order to determine the torques, both the pressure generating piston and the normalizing valve were considered.

The forces required by the pressure piston can be found by a free body diagram, as seen in figure 14:

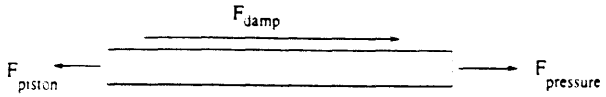

Figure 14: Piston free body diagram

In the figure, Fpiston is the force generated by the motor to drive the piston, Fdamp is viscous damping resulting from piston motion, and Fpressure is the force created by the chamber pressure acting on the piston face. Fdamp and Fpressure are defined as:

$$F_{damp} = c\dot{x} \tag{12}$$

$$F_{pressure} = P\pi r^2 \tag{13}$$

where c is the damping constant (assumed to .1 Ns/m), $\dot{x}$ is the velocity of the piston given by equation 8c, P is the time variant chamber pressure, approximated by a cosine wave of stroke dependent amplitude, and r is the piston radius.

From Newton's Second Law, the sum of these forces yields the acceleration of the piston shaft:

$$m_1\ddot{x} = F_{piston} - F_{damp} - F_{pressure} \tag{14}$$

m1 is the mass of the piston, and $\ddot{x}$ is its acceleration, found by time derivative of 8c. Therefore, the required motor force needed to drive the piston assembly can be found.

To translate this force into the torque on the motor shaft, the fulcrum must be found through geometric considerations, as revealed in figure 15. The fulcrum, r1, is

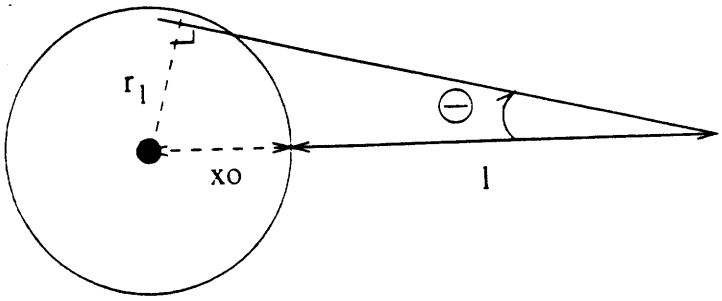

Figure 15: Fulcrum

given by:

$$r_1 = (x_0 + l)\sin\Theta \qquad (15)$$

where xo is the radial offset, l is the initial length of the piston from the flexible hinge to the aluminum disc, and Θ is the time variant angle between the nominal piston position and that at any given time. Since the piston cycles at a constant frequency, Θ is given by:

$$\Theta = \tan^{-1}\left(\frac{x_0}{x_0 + l}\right)\sin(2wt) \qquad (16)$$

Finally, the piston torque, Tpiston is determined by:

$$T_{piston} = F_{piston} r_1 \qquad (17)$$

With this, the valve torque must be considered.

The forces needed to actuate the valve arise from spring, inertial, and dissipative forces. The spring force generated by the 986 Nm compressive spring is simply:

$$F_{spring} = ky \tag{18}$$

in accordance with Hooke's Law, where y is the compression of the spring, described by the displacement function given in figure 12. The displacement function can be approximated by the equations:

$$\begin{aligned} &0 \le w < \pi :: y = .0035\cos 2wt + .0035 \\ &\pi \le w < 2\pi :: = .007 \end{aligned} \tag{19}$$

The spring force, Fspring, holds the cam and cam follower in contact, resulting in the principle dissipative force, Ffriction. This coulombic friction is proportional to the contact force (Fspring), and is therefore:

$$F_{friction} = \mu F_{spring} \tag{20}$$

In the equation, μ is the frictional coefficient between the aluminum cam and plexiglass cam follower (determined experimentally to be .15).

Finally, the inertial term of the valve shaft must be considered. As seen in the piston derivations, the inertial force is

$$F_{inertia} = m_2 \ddot{y} \tag{21}$$

where m2 is the mass of the valve shaft and cam follower, and $\ddot{y}$ is the acceleration found by the second time derivative of equation 19. However, since there is no definitive connection between the cam and the follower, the motor can only provide positive accelerations (extending the valve), while the retractive accelerations are provided by the compressive spring. Therefore, only the period $\pi / 4 \le \omega \le 3\pi / 4$ need be considered in the inertial force calculations.

As in the piston derivations, the fulcrum arm upon which these forces act must be determined in order to find the required motor torque. Both Finertia and Fspring act on the arm, r2, indicated in figure 16. r2 is derivable by:

$$r_2 = z \sin \phi \tag{22}$$

where ϕ is the position variant pressure angle seen in figure 11a, and z is the distance from the cam center to the contact point. z is related to the displacement, y, through addition of the base circle (. 3 cm).

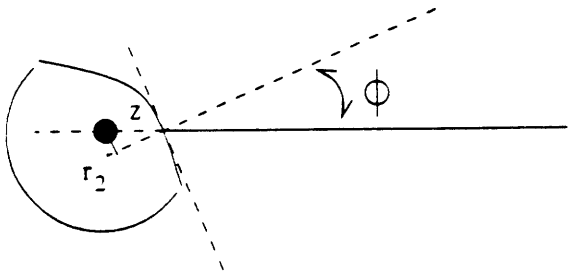

Figure 16: Valve fulcrum arm

The arm which the frictional force acts on can be approximated by z since the cam surface curvature is slight.

Therefore, the torque required to operate the valve system, Tvalve is given by

$$T_{valve} = (F_{spring} + F_{valve})r_2 + F_{friction}z \tag{23}$$

and the total torque needed to drive the ventilator is

$$T_{total} = T_{piston} + T_{valve} \tag{24}$$

In these derivations, the bearing and motor damping are assumed to be negligible in relation to the other components. Also, since the ventilator operates at a constant velocity, the transient factors (such as the motor inertia) were not considered.

The theoretical torques required over a given cycle are plotted in figures 17 a and b for various ventilator operation setups. The solid line in 17*a* indicates normal ventilation at a frequency of 2 Hz and a pressure swing of 25 cm H20. The torque profile is dominated by spring force considerations, as is witnessed by the torque flips when the spring goes from a compressive to an extensive state. This spring dominance at low frequencies was the reason the valve was designed to run smoothly at about 50 Hz instead of 100 Hz. Doubling the frequency would quadruple the spring force. Therefore, there would be excessive power loss even though the ventilator would rarely be run at such high frequencies.

As the frequency is increased, the inertial elements become more relevant. The dashed line in 17a reveals a sample at 20 Hz with 25 cm H20 pressure generation. The distinctive peaks are smoothed by the accelerations and decelerations of the shafts. Such operation (high frequency, high pressure) would severely over-ventilate the neonatal mice. Therefore, the solid line in 17b, shows a more realistic 20 Hz trial with a 5 cm H20 pressure variation. Again, since this is accomplished by reducing the stroke length, the accelerations of the piston are not as great and the inertial term is minimized, yielding a plot similar to the normal ventilation trial in 17a. Finally, the dashed line in 17b shows an example at the maximal frequency of 100 Hz, where again, the inertial terms can be seen. In each figure, there is a constant offset from 0 Nm (witnessed at positions $> \pi$), which is a result of the friction between the cam and cam follower.

By finding the peak and minimum torques, the limiting bounds were determined to be between .1 Nm to -0.06 Nm. Since there is a considerable amount of variation in the

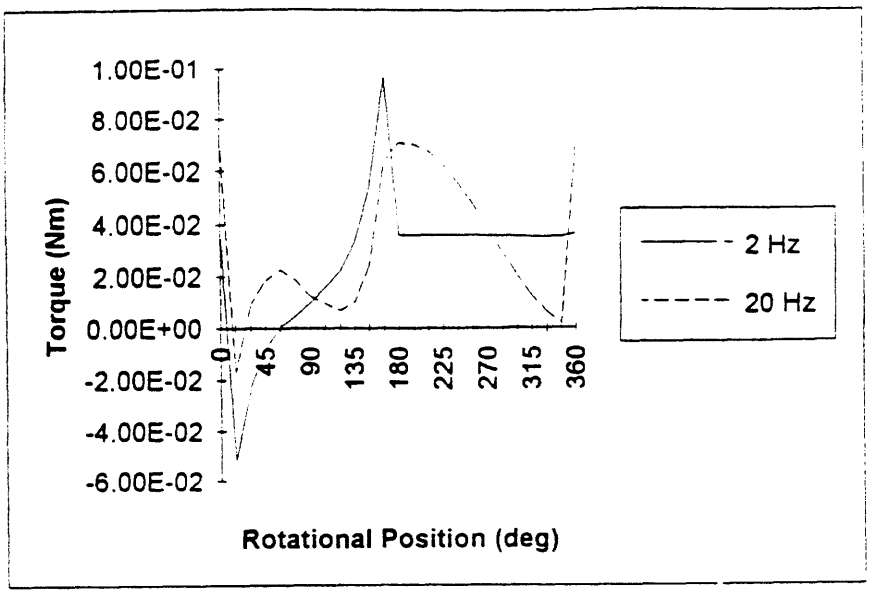

Figure 17a: Torque variance for 25 cm H20 pressure generation.

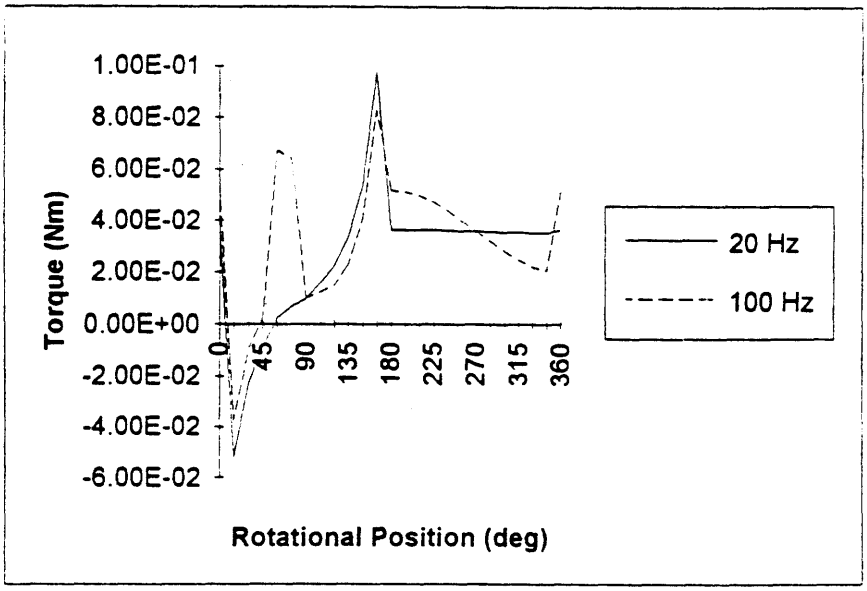

Figure 17b: Torque variance for 5 cm H20 pressure generation.

torque, either a high inertia system with nominal feedback or a high torque motor with good feedback can be used to provide a constant rotational velocity. The inertia method, acting as a torque buffer, would be efficient and operate well at high frequencies. However, such a system would only work at low frequencies if an extremely high rotational inertia was used, and therefore is impractical. The high torque motor with feedback and a small mechanical time constant is more suitable to this application considering the wide frequency range. In order to ensure the motor's capability to drive the ventilator smoothly, a maximum continuous torque of at least three times the torque variance was used in motor selection.

In order to provide this torque, several types of motors were considered: DC brush, DC brushless, and AC inductance motors. The AC induction and DC brushless had the advantage of wear resistance. Since neither had brushes their operation time was limited by bearing life. However, the AC induction motor is much more difficult to control than with simple tachometer feedback. Similarly, the DC brushless motor is much more complex to control, and therefore considerably more expensive than a brush motor with similar torque and frequency characteristics.

Since it is possible to replace worn brushes, the life span was less of an issue than price and complexity. After looking at several possibilities, the KOLLMORGAN U9M4T DC servobrush motor was selected (estimated to have a brush life of over year under continuos operation under maximal stress). A torque vs. frequency graph for the motor is shown in figure 18. As seen, the motor can operate continuously over a range from 0 to 4000 rpm (67 Hz), providing a torque of around 40 oz in (.28 Nm) with no ventilation. If

cooling or non-continuous operation is an option, the torque can be increased by quite a margin. Additionally, since the 4000 rpm is achievable at under 30 V, and the KXA-48 is a 48 volt amplifier, speeds of 100 Hz can be easily reached, though there is a slight drop in torque (.77 ozin/KRPM as given in the data sheet).

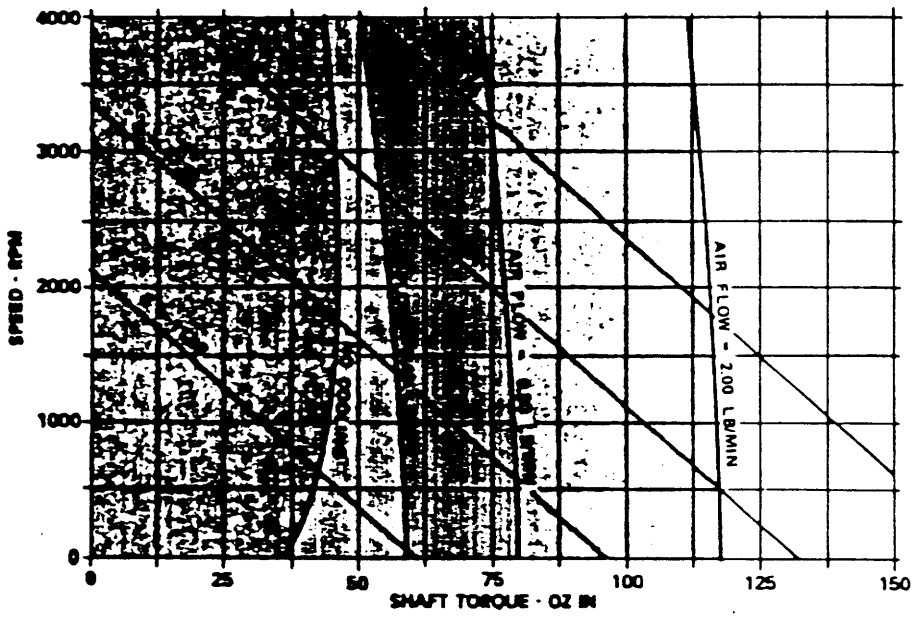

Figure 18: Torque vs. Frequency characteristics of U9M4T

(A complete data sheet is included in Appendix C.)

To control the motor, an integrated tachometer with an output voltage of 2.25 V/KRPM is used. This tachometer provides a feedback signal to the KXA-48 amplifier, set in a velocity control mode (as opposed to torque control), which in turn drives the motor. The amplifier switching frequency is 40 kHz, well beyond the need for this application. The motor has a mechanical time constant of 20.5 msec. Though this yields a lower than desired frequency of around 50 Hz (ideally, it would be 4 times the desired

controllable frequency if simple feedback is used), the required 100 Hz can be achieved via the KXA phase adjust control strategy [11].

2.5 Mouse Chamber

2.5.1 Description

A schematic of the mouse chamber can be seen in Figure 19. The mouse chamber is made of two compartments. The first is a 3 ml plastic cylinder which is detachable from the apparatus. It is connected via a three way valve to the pressure generating piston assembly. The unconnected end allows a neonatal mouse to be positioned inside the cylinder. To stop leakage, a rubber cuff is first placed around the newborn's neck, and

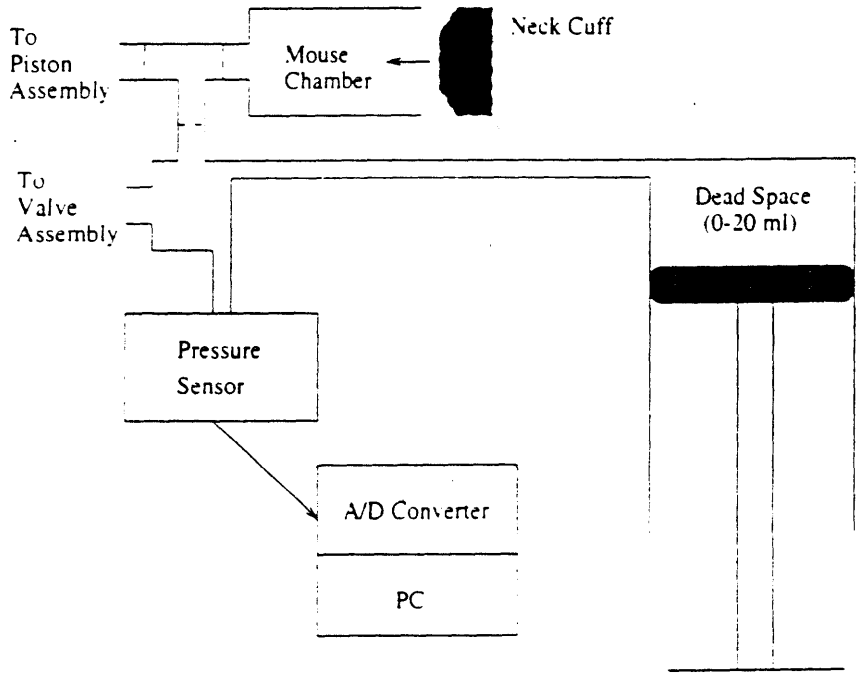

Figure 19: Schematic of mouse chamber

then sealed with a dental adhesive. Then, the mouse's body is placed within the chamber, with the rubber fitting snugly in place.

A second compartment is connected to the third stem of the three way valve, and houses the chamber end of the normalizing valve. This compartment has an adjustable volume of 20 ml which acts as a dead space. By varying the volume, the mouse chamber pressure can be varied while the ventilator is in operation, though to achieve the large pressure variations, the stroke length must be adjusted.

A silicon sensor (Motorola MPX 2010) is connected to the chamber and allows for a real time pressure signal to be monitored (either on oscilloscope or computer).

2.5.2 Methodology

The required size of the mouse chamber was determined in conjunction with the pressure generating piston design. The design required a chamber volume of 15 ml, considering the parameters chosen (piston dimensions and stroke length). The actual chamber is adjustable from approximately 5 ml (3 ml mouse chamber plus 2 ml connection tubes) to 25 ml. This wide range was selected since the theoretical model assumes that leakage occurs only through the piston gap. In reality, other sources (such as the neck cuff) may be present. Therefore, a variable volume allows for pressure calibration. Additionally, the adjustable volume allows for the ventilator pressures to be varied while in operation, since stroke length adjustment requires the motor to be stopped. Finally, the large dead space, as determined empirically, successfully negates the pressure fluctuations created by the valve operation.

Chapter 3

Performance

3.1 Mechanical Operation

The ventilator specifications were to deliver pressures from 0 to 25 cm H20 over a frequency range of 1 to 100 Hz. This range was tested by sealing the mouse chamber orifice with a stopper and collecting pressure profile samples via an A/D converter and PC. Figure 20 shows low frequency ventilator operation at a 4 Hz frequency and a pressure swing of 22.5 cm H20. The normalizing valve function can be seen by the flat regions in the pressure profile when a positive pressure would otherwise be generated. Figure 21 shows the pressure wave form at a frequency of 40 Hz and a pressure fluctuation of 3.5 cm H20, qualifying as very high frequency ventilation. Again, the normalizing valve effectively keeps the baseline pressure from drifting, though the line is noisy due in part to systemic vibrations.

As mentioned in the valve design section, the 986 N/m spring is capable of handling frequencies up to about 50 Hz (some considerations must be made for the damped natural frequency). As the system is pushed past this point, the cam and valve become unsynchronized. The effect of this error can be witnessed through the positive pressures generated in figure 22, which shows a trial at 100 Hz. Though this is an undesirable occurrence, it is acceptable so long as volume generation is minimal as discussed in the introduction.

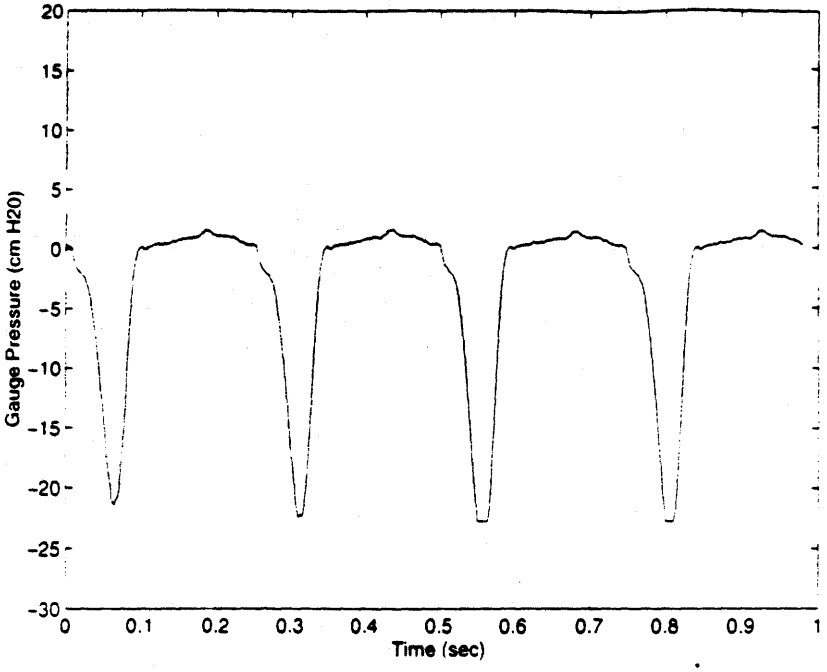

Figure 20 Pressure profile for low frequency, high pressure operation (4 Hz/ 22.5 cmH20)

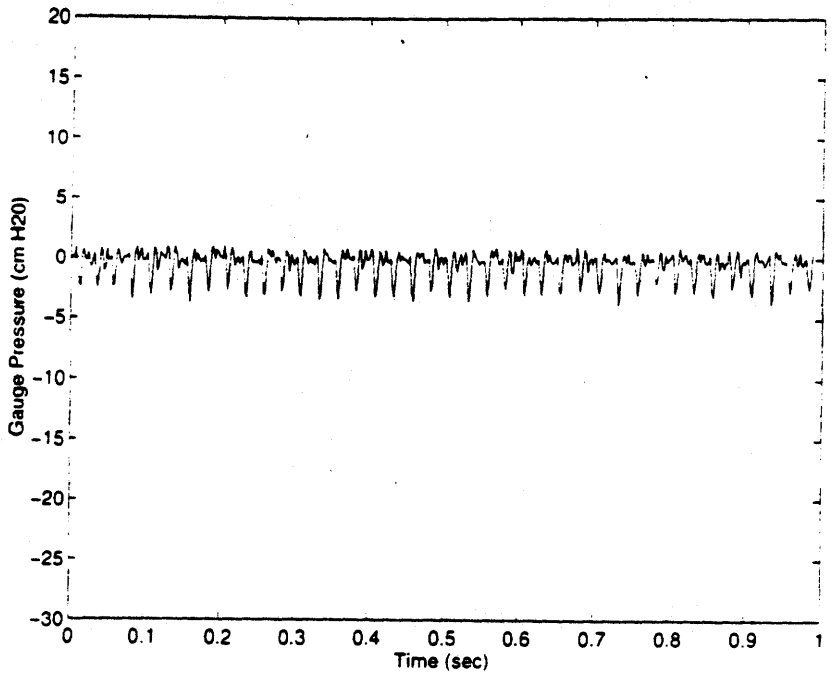

Figure 21:Pressure profile for high frequency, low pressure operation (40Hz / 3.5 cmH20)

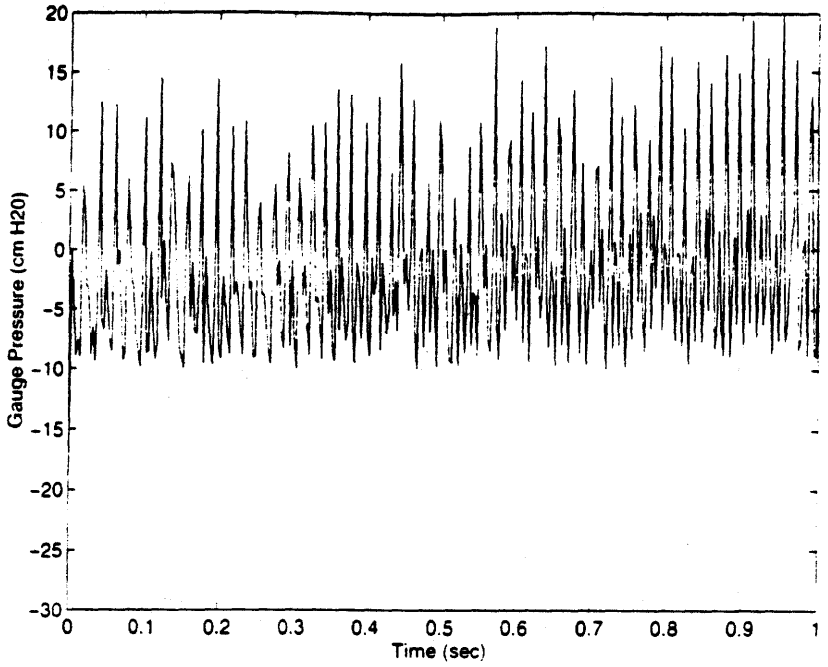

Figure 22: Pressure profile for 100 Hz operation revealing valve malfunction

The need for the normalizing valve is witnessed in figure 23, which reveals the baseline drift as predicted in the theoretical simulations. At 0.4 sec, the valve was plugged and the resultant steady shift in the baseline can be seen. A new equilibrium is reached after 0.3 sec. This small time constant indicates that there are other sources of leakage in the system apart from the modeled gap. Furthermore, as the valve is plugged, the amplitude of the pressure swing increases, showing that the valve is one such source.

The function of the 20 ml dead space can be seen in figure 24. The connection to the 20 ml dead space was clamped until .7 sec. At this point, the line was open and the resulting drop in pressure can be seen. Under the given conditions, the pressure is nearly halved. As discussed, this mechanism can be used in pressure calibrations and adjustments while the ventilator is in operation.

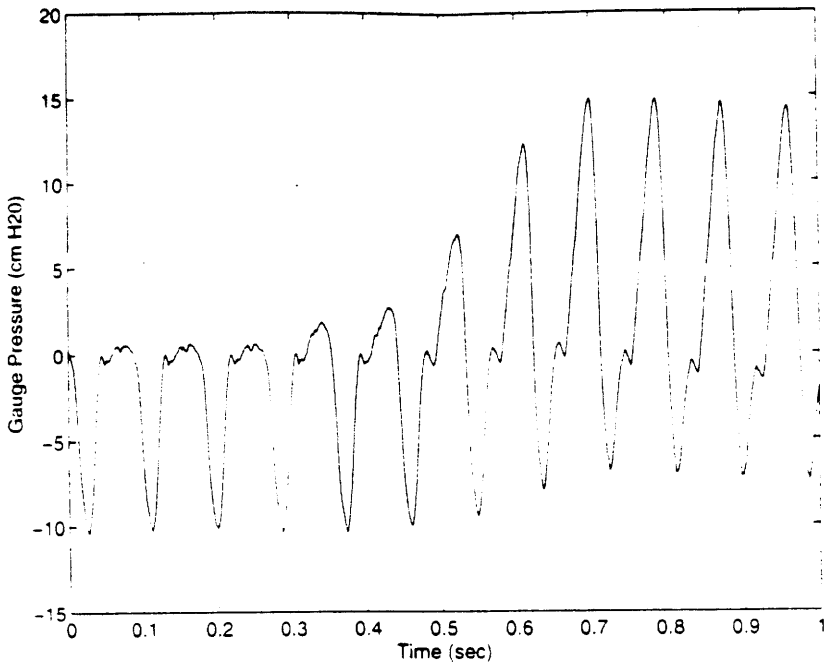

Figure 23: Sample pressure plot with clogged normalizing valve indicating baseline drift

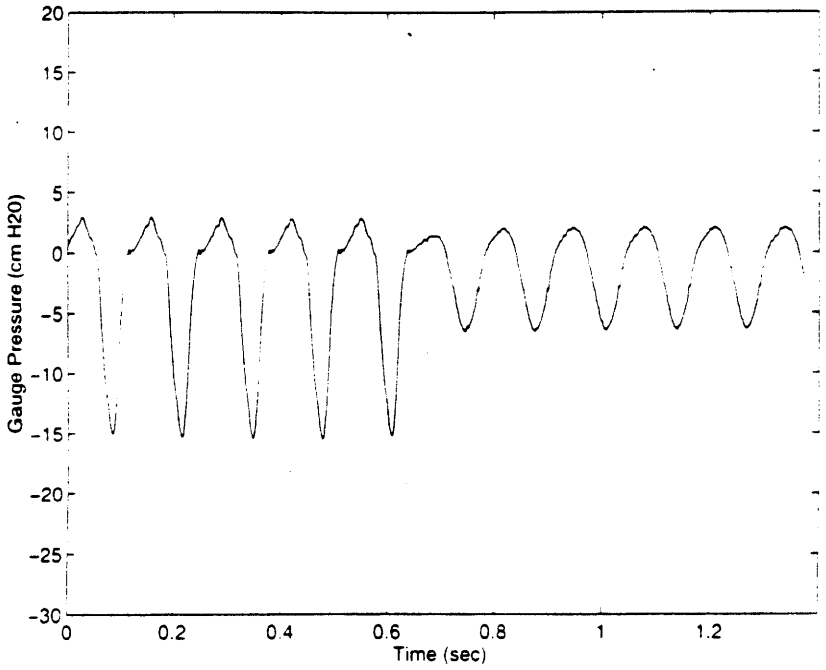

Figure 24: Pressure profile fluctuation with dead space change

Overall, the mechanical performance of the ventilator seems to be adequate. The pressures can be varied over a wide frequency range allowing both for normal and high frequency modes of ventilation. Though proper function is not achievable at frequencies much greater than 50 Hz with the current spring, this drawback allows a significant amount of power to be saved. However, if frequencies much higher than 50 Hz are desired, the spring can accordingly be changed.

3.2 In-vivo testing

Actual ventilator testing has been performed on both normal control and mutant mice. The primary use of the controls was to ensure that the ventilator was not harming the mice. Figure 25 shows a sample recording on a newborn mouse (10 Hz/ 5 cm H20). The preliminary goal of these tests was to ascertain if the ventilator could prolong the lives of the mutants. As expected, the control mice lived regardless of ventilatory assistance.

Two liters containing mutants were tested on the ventilator. In each trial, one mutant was placed in the device and the remainder mutant littermate was used as a control. Frequencies between 10 and 20 Hz were used with pressure swings of around 6 cm H20 for these trials. Figure 26 compares the life spans of the ventilated and non-ventilated mice. The total span is divided into ventilator and post-ventilator periods. Also, the maximum life span (20 hrs) of unventilated mice is given as a limit on the graph.

The figure clearly shows that the life span of the mutants seems to be prolonged with respiratory assist. In both instances, the ventilated mice outlived their littermate controls, and furthermore, broke the previous life span .boundary set at 20 hours. In fact,

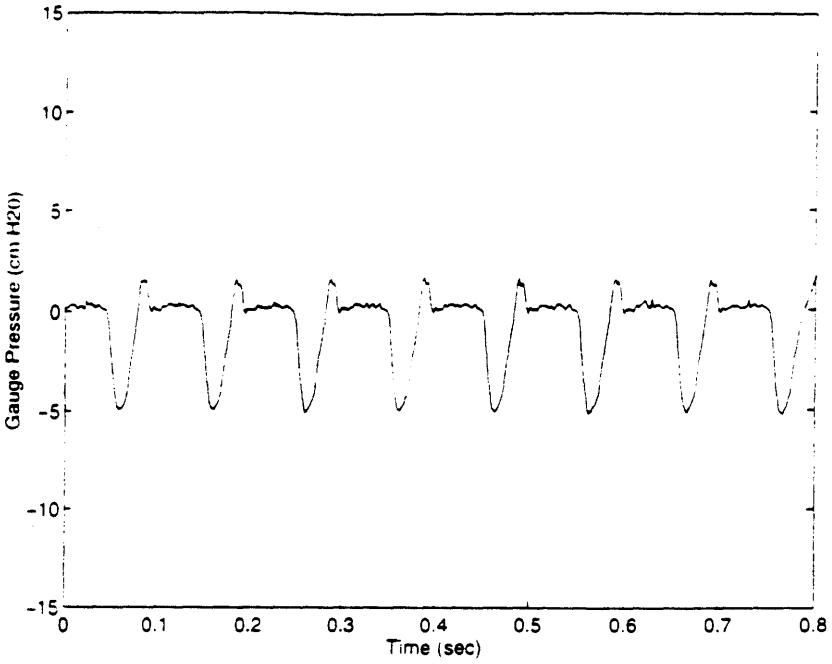

Figure 25: Pressure profile of typical in-vivo recording (10Hz,5cm H20)

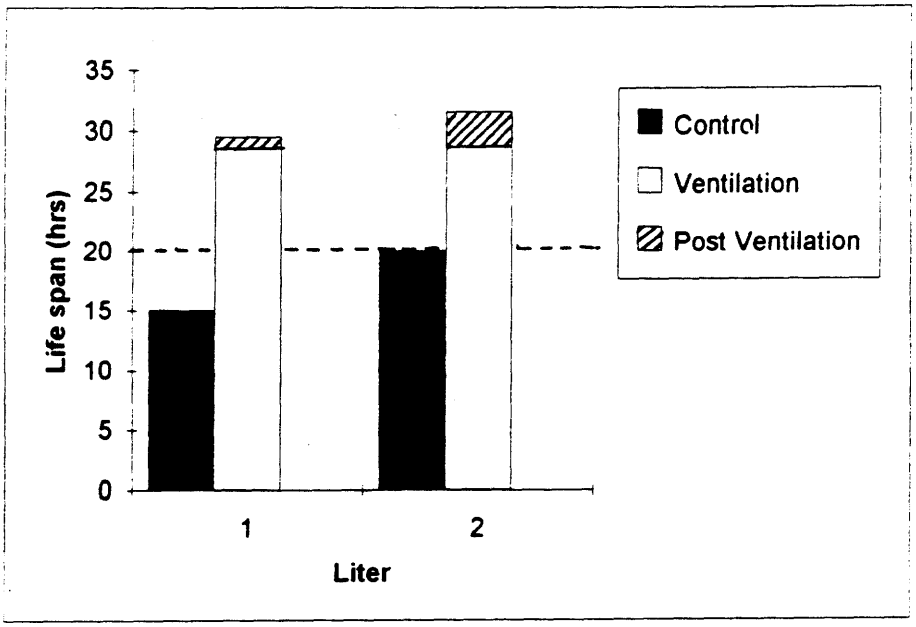

Figure 26: Life span of mutants and control littermates

the only reason that the ventilated mutants did not survive longer was that they were deliberately taken off the ventilator in order assess their unsupported survivability.

A possible explanation for the eventual death of the ventilated mice is starvation. As mentioned before, the mutants have several abnormalities, including an inability to suckle milk. Therefore, they are not fed from the time of birth and are severely malnourished (even normal mice cannot survive long without food).

The short post-ventilator life of the first mutant, also indicates that the ventilator may train the mice to cease spontaneous breathing. Apparently, after being taken off the ventilator, the mutant did not re-start the process and died. Ventilator training is a major concern in human respiration. After being on a ventilator for a prolonged period of time, patients must undergo a weaning process in order to resume self-initiated breathing. If this is indeed the case, a similar strategy may have to be adopted for the mice.

One question that remains to be answered is whether the respiratory failure is caused by systemic organ failure or central nervous system (CNS) malfunctioning due to NMDA receptor deficiency. Currently, lung pathology experiments are being performed on the mutant mice to see if the lungs can be preserved through ventilation, thereby indicating a CNS malfunction.

Regardless, many more tests must be performed to fully understand the proper techniques and role of mechanical ventilation in the neonatal mice.

Chapter 4

Conclusions

4.1 Summary

The need for a mechanical ventilator for newborn mice has arisen from NMDA knockout mice. This genetic alteration affects the mice in various ways including respiratory distress. The malfunction is believed to result in respiratory failure leading to the premature death of the newborn animals, thereby impeding further investigative efforts into the role of the NMDA receptors in neural development.

Ventilatory assist was chosen as a means of foregoing respiratory failure in hopes of sustaining the mutant mice. Previous ventilator designs do not allow for respiratory assist on such a small scale. Therefore, a high frequency negative pressure ventilator was designed.

The ventilator is unique in several ways. Since the device can achieve a wide spectrum of pressure fluctuations over a large frequency range, it is effective in both normal and high-frequency ventilation modes. This flexibility is needed since newborns of this nature have never been ventilated and the proper techniques and parameters are not known. Additionally, the double piston design (pressure piston and valve piston) elegantly normalizes the chamber pressure, allowing negative pressures to be generated efficiently. The valve mechanism also keeps positive pressures from building around the body surface, which would be detrimental to respiratory efforts.

Preliminary studies have indicated that the life span of the ventilated mutant mice can be prolonged by more than 10 hrs. Still, many more studies must be performed to

ascertain the proper ventilatory parameters for such newborn mice and the physiological consequences of mechanical ventilation.

4.2 Future Considerations

As seen in the performance section, the valve is malfunctional at extremely high frequencies. In future designs, the spring constant can be varied to the full 3950 N/m to allow valve synchronization at 100 Hz. An alternative method to achieve similar results, yet minimize power consumption, is to reduce the weight of the cam shaft. However, before either option is fully considered, the effective ventilation range for the newborn mice should be determined.

Furthermore, at various frequencies (multiples of the inherent natural frequency of the ventilator structure), vibration occurs, causing extraneous fluctuations as seen in figure 21. The forcing is a result of mass imbalances on the rotating mass. Though this vibration has not posed a serious problem, future attempts to perhaps make neural recordings while keeping ventilitory assistance may not be possible with such vibrations. To minimize the damping, the mass can be counterbalanced, or a vibrational damper can be designed for the ventilator.

Also, the current method of negative pressure ventilation requires that a cuff be place around the neck of the newborn animal. Although this technique is much less invasive than a tracheotomy, it still has the risk of closing the subjects airway's, increasing the resistance to flow. Another option is to place the cuff around the body, and simply

oscillate the mouse's abdomen. Previous studies have shown this to be an extremely effective method of negative pressure ventilation [12].

Another consideration is temperature control over the mouse chamber. Currently, unventilated mice are kept in an incubator since their homeostatic mechanisms are not adequate at such a young age. However, the present design does not account for this problem.

Furthermore, as mentioned in the pressure generating piston section, positive pressures serve to close the airways, whereas negative pressures open them. Therefore, a negative pressure source connected to the outlet of the normalizing valve would create a negative end expiatory pressure, helping to open the airways. This strategy has been employed in modern positive pressure ventilators (positive end expiatory pressure) and helps to negate the effects of airway resistance.

4.3 Concluding Remarks

The miniature HF ventilator discussed in this paper is an excellent stepping stone in the respiration of the NMDA mutants, as well as any incapable newborn mice suffering from respiratory failure. Various changes could further the effectiveness of the device. Regardless, the use of the ventilator has been shown to increase the life spans of tested mutant mice, and additional studies are currently being performed to support these initial findings.

Appendix A: Respiratory Mechanics Model (qbasic)

```
vdes=.04
tol=.001
phigh=40
plow=0
screen 2,1
REM parameters
po=(phigh+plow)/2
w=1
dt=.01/w
w=w*2*3.1415
REM Constants
r=2.314
e=554
tme=1

start:
        LOCATE 1,1:PRINT po, vhigh
        REM Initial Conditions
        vo=0
        f=0
        vhigh=0

        FOR t=0 TO tme STEP dt
                p=-po/2*COS(w*t)+po/2
                v=(p-r*ABS(f))/e
                f=(v-vo)/dt
                vo=v

                IF v>vhigh THEN vhigh = v
        NEXT t

        IF (vhigh-vdes)>tol THEN
                phigh=po
                po=(phigh+plow)/2
        ELSE
                plow=po
                po=(phigh+plow)/2
        END IF

GOTO start
```

Appendix B: Piston Model (MATLAB)

```
function dy=model(t,y)
m=y(1);                          mass
p=y(2);                          pressure
x=y(3);                          position

;PARAMETERS
r1=.00245;                       shaft radius
r2=.00255;                       cylinder radius
l=.05;                           nominal gap length
vmin=15e-6;                      minimal chamber volume
xo=.03                           stroke length

;CONSTANTS
R=287;                           gas constant (air)
k=298;                           temperature
u=1.82e-5;                       viscosity (air)
b=1.204;                         density (air)
pa=1e5;                          atmospheric pressure

xmax=.03;                        max stroke length
a=pi*r1^2;                       piston area
h=r2-r1;                         gap
vc=((xmax-xo)/2)*pi*r2^2+vmin;     extra pisotn volume

;DIFFERENTIAL RELATIONS
dx=w*xo/2*sin(w*t);
dm=2*b*pi*r1*((dx*h/2)-(h^3)*(p-pa)/(12*u*(xo)+l-x)));
dp=(dm*R*k-a*p*dx)/(a(*x+vc);

dy(1)=dm;
dy(2)=dp;
dy(3)=dx;
```

Appendix C: Motor Specifications

U-SERIES Motors With Integral Tachometers (9)

	MOTOR PERFORMANCE INCREMENTAL MOTION CONTROL	SYMBOL	UNIT	U6M4T	U9M4T	U9M4HT
1.1	PEAK TORQUE (1)	TP	OZ IN	162.9	434.0	664.9
1.2	CONTINUOUS STALL TORQUE	[illegible]	[illegible]	14.5	[illegible]	[illegible]
1.3	PEAK CURRENT (1)	IP	AMPS	43.6	72.0	72.9
1.4	CONTINUOUS STALL CURRENT	[illegible]	AMPS	4.10	6.81	[illegible]
1.5	PEAK ACCELERATION WITHOUT LOAD (1) (5)	AP	KRAD/SEC SEC	130.3	52.3	80.1
1.6	COGGING TORQUE	[illegible]	OZ IN.	[illegible]	[illegible]	
2.0	**MOTOR PERFORMANCE: RATED (2)**					
2.1	TORQUE	[illegible]	OZ IN.	16.2	45.9	71.4
2.2	SPEED	N	RPM	3000.0	3000.0	3000.0
2.3	POWER OUTPUT	P	WATTS	36.0	101.7	158.6
2.4	TERMINAL VOLTAGE	E	VOLTS	16.7	22.9	29.9
2.5	CURRENT		AMPS	4.65	9.63	9.51
2.6	NO LOAD SPEED AT RATED VOLTAGE	NM	RPM	5425.6	4593.1	4077.4
2.7	MAX PERMISSIBLE DISSIPATON AT RATED SPEED (3)	PL	WATTS	41.7	96.2	96.2
3.0	**MOTOR CONSTANTS: INTRINSTIC (AT 25 DEG C)**					
3.1	TORQUE CONSTANT	KT	OZ IN/AMP	3.76	5.09	9.30
3.2	BACK EMF CONSTANT	KE	VOLTS/KRPM	2.78	4.50	6.87
3.3	TERMINAL RESISTANCE (7)	RT	OHMS	1.320	0.950	0.950
3.3.1	ARMATURE RESISTANCE	RA	OHMS	1.070	0.660	0.660
3.4	AVERAGE FRICTION TORQUE	TF	OZ IN	1.0	4.5	4.5
3.5	VISCOUS DAMPING CONSTANT	KD	OZ IN/KRPM	0.10	0.84	1.29
3.6	MOMENT OF INERTIA	JM	OZ IN SEC/SEC	0.00125	0.00830	0.00850
3.7	ARMATURE INDUCTANCE	L	MICRO HENRY	<100.0	<100.0	<100.0
3.8	TEMPERATURE COEFF OF KE	C	%/DEG C RISE	-0.02	-0.02	-0.02
3.9	NUMBER OF COMMUTATOR BARS	Z		94	117	117
3.10	NUMBER OF POLES OF MAGNETIC FIELD	PF		6	9	9
4.0	**MOTOR CONSTANTS: DERIVED (AT 25 DEG C)**					
4.1	MECHANICAL TIME CONSTANT WITHOUT LOAD	TM	MILLISEC	13.25	20.52	9.56
4.2	ELECTRICAL TIME CONSTANT	TE	MILLISEC	<0.09	<0.15	<0.15
4.3	SPEED REGULATION AT CONSTANT TERM VOLTAGE	RM	RPM/OZ IN	101.24	23.61	10.20
5.0	**THERMAL RESISTANCE**					
5.1	MOUNTED ON ALUM HEAT SINK (8"x16" x 3/8")					
5.1.1	ARMATURE TO AMBIENT AT STALL	RAA	DEG C/WATT	4.04	2.40	2.40
5.1.2	ARMATURE TO AMBIENT AT 3000 RPM	RAA	DEG C/WATT	3.00	1.30	1.30
5.2	FORCED THROUGH-AIR COOLED (6)					
5.2.1	ARM TO AMB WITH AIR FLOW OF .4 LBS/MIN	RAA	DEG C/WATT	1.40	1.05	1.10
5.2.2	ARM TO AMB WITH AIR FLOW OF .8 LBS.MIN	RAA	DEG C/WATT	0.91	0.61	0.65
5.2.3	ARM TO AMB WITH AIR FLOW OF 2.0 LBS/MIN	RAA	DEG C/WATT	0.54	0.30	0.32
6.0	**ANALOG TACHOMETER CHARACTERISTICS (AT 25 DEG C)**					
6.1	OUTPUT VOLTAGE	V	VOLTS/KRPM	1.39	2.25	3.43
6.2	RIPPLE VOLTAGE MAX, PEAK TO PEAK (8)					
6.2.1	AT 1000 RPM	VRH		3.0	3.0	3.0
6.2.2	AT 500 RPM	VRM	%	3.5	3.5	3.5
6.2.3	AT 100 RPM	VRL		4.5	4.5	4.5
6.3	LINEARITY OF OUTPUT VOLTAGE (REF. 3600 RPM)	LIN	%	0.06	0.06	0.06
6.4	BI-DIRECTIONAL TOL. (DIFF. IN OUTPUT VOLTS /KRPM)	BI		1.0	1.0	1.0
6.5	OUTPUT IMPEDANCE, RESISTIVE	R	OHMS	0.504	0.370	0.370
6.6	TEMPERATURE COEFF OF V	[illegible]	%/DEG C RISE	-0.02	-0.02	-0.02
6.7	MOMENT OF INERTIA: INCLUDED IN ITEM 3.6					
6.8	LOAD RESISTANCE RECOMMEND MIN	RL	OHMS	504.0	370.0	370.0
6.9	NUMBER OF COMMUTATOR BARS	ZT		94	117	117
7.0	PHYSICAL CHARACTERISTICS					
7.1	MOTOR DIAMETER	D	IN	2.87	4.37	4.37
7.2	MOTOR LENGTH	LG	IN	2.03	1.86	2.41
7.3	MOTOR WEIGHT	W	LBS	1.80	4.50	5.30

NOTES:

(1) These are based upon the least of the demagnetization limit, the structual limit and the thermal limit. It is calculated for maximum pulse duration of 50 millisec and 1% duty cycle.

(2) All values are based upon 150° C. armature temperature.

(3) Maximum Permissible Dissipation = speeds and torques are achievable as armature temp. is kept below 150° C. Continuous speed beyond 4000 RPM is not recommended. Consult PMI Motors for other speed ratings.

Bibliography

1. Li Y, Erzurumlu RS, Chen C, Jhaveir S and Tonegawa S. Whisker-related neuronal patterns fail to develop in the trigeminal brainstem nuclei of NMDAR1 knockout mice. *Cell* **76**, 427-437 (1994).

2. Forrest D, Yuzaki M, Soares H D et al. Targeted disruption of NMDA receptor 1 gene abolishes NMDA response and results in neonatal death. *Neuron* **13**, 325-338 (1994).

3. Poon C-S, Li Y, Li S-X and Tonegawa S. Respiratory rhythm is altered in neonatal mice with malfunctional NMDA receptors. *FASEB J* **8**, 2252 (1994).

4. Harf A, Bertrand C, and Chang H K. Ventilation by high-frequency oscillation of thorax or at trachea in rats. *Journal of Applied Physiology* **56(1),** 155-160 (1984).

5. Poon C-S, Ward S A. A device to provide respiratory mechanical unloading. *IEEE Trans Biomed Engineering* **BME-33** 361-364 (1986)

6. Poon C-S, Li S-X, Kolandaivelu K, Vreeland P, Frantz III ID. Comparison of negative impedance ventilation and pressure support in an alveolar lavage model. *American Journal of Respiratory and Critical Care Medicine* **149(4)**, A66 (1994).

7. Bohn D J, Miyasaka K, Marchak B E, Thompson W K, Froese A B, Bryan A C. Ventilation by high frequency oscillation. *Journal of Applied Physiology* **48(4)**, 710-716, (1980).

8. Stahl W. Scaling of respiratory variables in mammals. *Journal of Applied Physiology* **22(3)**, 453-460 (1967).

9. Fay, J A. Fluid Mechanics Class Notes. Cambridge: MIT, 1994.

10. Jensen C, Helsel J. Engineering Drawing and Design. 3rd ed. New York: McGraw-Hill Book Company. 1985.

11. PMI Motion Technologies. Operating Instructions: PMI Amplifiers/ KXA Series. ver 1.02 rev A. New York: PMI Motion Technologies, 1991.

12. Fuyuki T, Suzuki S, Sakurai M, Sasaki H, Butler J P, Takishima T. Ventilator effectiveness of high-frequency oscillation applied to the body surface. *Journal of Applied Physiology* **62(6)**, 2410-2415 (1987).